RESEARCH Open Access

## Check for updates

# Proteomic insights into platelet dysregulation and pathogenic mechanisms of chronic thromboembolic pulmonary hypertension

Lu Sun<sup>1,2</sup>, Haobo Li<sup>1,2</sup>, Yuhan Li<sup>1,2</sup>, Xincheng Li<sup>2</sup>, Han Tian<sup>2</sup>, Jixiang Liu<sup>2</sup>, Min Liu<sup>3</sup>, Jinzhi Wang<sup>4</sup>, Qiang Huang<sup>2</sup>, Zhu Zhang<sup>2</sup>, Xiaofan Ji<sup>1,2</sup>, Linfeng Xi<sup>2,5</sup>, Kuangxun Li<sup>1,2</sup>, Yishan Li<sup>2,6</sup>, Ximei Niu<sup>2,7</sup>, Mengjie Duo<sup>1,2</sup>, Bingzhang Zou<sup>1,2</sup>, Jing Wen<sup>1,2</sup>, Jie Li<sup>2,8</sup>, Ran Miao<sup>2</sup>, Wanmu Xie<sup>2</sup>, Shiqing Xu<sup>8\*</sup>, Peiran Yang<sup>9\*</sup> and Zhenguo Zhai<sup>2\*</sup>

### **Abstract**

**Background** Undissolved thrombus blocks the pulmonary arteries in chronic thromboembolic pulmonary hypertension (CTEPH), a potentially fatal illness that raises pulmonary resistance, causes right heart failure, and even results in death. Although platelets are linked to vascular dysfunction and thrombus formation, it is yet unknown what precise proteome alterations and mechanistic roles they play in CTEPH.

**Methods** We extracted platelet-rich plasma from peripheral blood and separated the plasma to obtain enriched platelet pellet (EPP). Quantitative proteomics was used to examine EPP from CTEPH patients and healthy controls using mass spectrometry. The relationship between protein levels and clinical markers of right heart function was examined. Platelet activity, morphology, and interactions with other blood components were evaluated using transmission electron microscopy, immunofluorescence, and flow cytometry.

**Results** The proteomic investigation found that 179 proteins were differentially expressed in CTEPH patients. The analysis revealed that these proteins were involved in crucial processes such as complement and coagulation cascades, phagosome, and neutrophil extracellular trap (NET) formation. Elevated proteins, specifically NOX2, PAD4, ITGB2, and HMGB1, have been associated to platelet-neutrophil aggregates and NET formation. In addition, enhanced P-selectin expression in platelets and plasma confirmed greater platelet activation in CTEPH patients. Notably, PAD4 and NOX2 levels showed a substantial correlation with hemodynamic parameters and right heart dysfunction. MPO-DNA, a NET marker associated with P-selectin and ITGB2 expression, was discovered in higher concentrations in CTEPH patients' plasmas.

**Conclusion** Platelet aggregation and activation in CTEPH encourage the formation of NETs, which advances the disease and prolongs thrombus. Right heart insufficiency and hemodynamic markers had a strong correlation with

\*Correspondence: Shiqing Xu xushiqing@163.com Peiran Yang peiran.yang@foxmail.com Zhenguo Zhai zhaizhenguo2011@126.com

Full list of author information is available at the end of the article

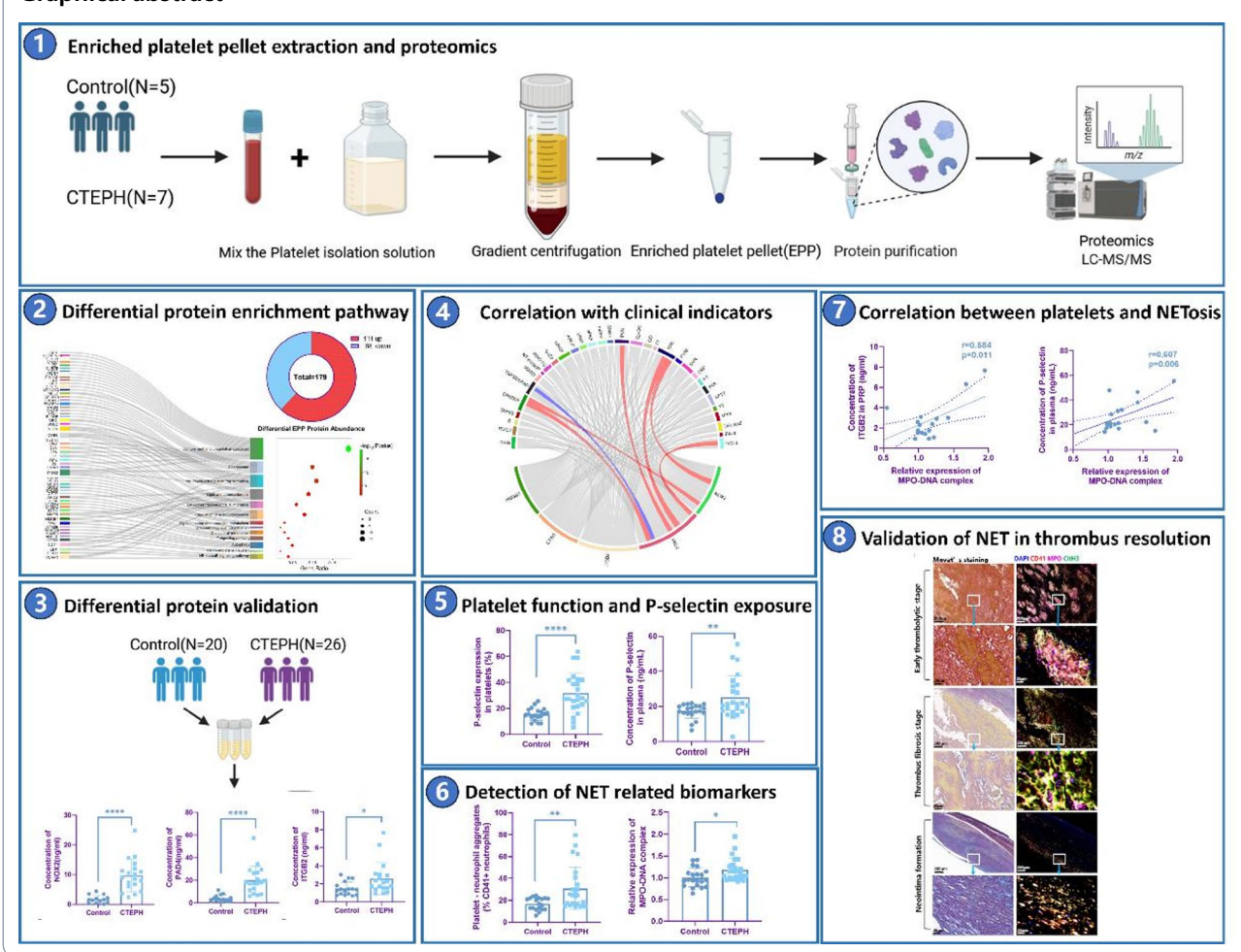


© The Author(s) 2025. **Open Access** This article is licensed under a Creative Commons Attribution-NonCommercial-NoDerivatives 4.0 International License, which permits any non-commercial use, sharing, distribution and reproduction in any medium or format, as long as you give appropriate credit to the original author(s) and the source, provide a link to the Creative Commons licence, and indicate if you modified the licensed material. You do not have permission under this licence to share adapted material derived from this article or parts of it. The images or other third party material in this article are included in the article's Creative Commons licence, unless indicated otherwise in a credit line to the material. If material is not included in the article's Creative Commons licence and your intended use is not permitted by statutory regulation or exceeds the permitted use, you will need to obtain permission directly from the copyright holder. To view a copy of this licence, visit http://creativecommons.org/licenses/by-nc-nd/4.0/.

PAD4 and NOX2 levels, indicating that these biomarkers may be employed to assess the severity and prognosis of CTEPH disease and offer a fresh approach to targeted treatment. The results highlight the need for additional study to elucidate platelet-mediated pathways and create therapies for CTEPH that target platelets.

**Keywords** Chronic thromboembolic pulmonary hypertension, Proteome, Enriched platelet pellet, Neutrophil extracellular trap, Delayed thrombus resolution

### **Graphical abstract**



### **Background**

Chronic thromboembolic pulmonary hypertension (CTEPH) is one of consequences of acute pulmonary embolism (PE) [1, 2]. Deep vein thrombosis (DVT) is a major cause of PE, with over half of individuals with proximal DVT (iliac, femoral, popliteal veins) developing PE [3–5]. When anticoagulation is started after acute PE revascularizes the majority of patients, 2.11% to 3.53% will develop CTEPH. Asian populations have a far higher incidence of this condition than European cultures [6–9]. For CTEPH, pulmonary endarterectomy (PEA) is still the only effective treatment [10]. Histopathological examination of PEA samples has revealed varying stages of acute and chronic thrombus, as well as differing patterns of thrombus resolution [11]. Impaired thrombus resolution

is thought to be a contributing factor in the pathogenesis of CTEPH [12, 13]. However, there are still some patients are unable to undergo treatment due to thrombotic complications or surgical contraindications, resulting in alteration of the pulmonary arteries and right ventricular dilation or failure, potentially culminating in death [1].

Platelets, which are tiny, non-nucleated cell fragments with a diameter of  $2{\text -}4~\mu m$ , are crucial for clotting and hemostasis [14]. In pulmonary hypertension, activated platelets generate highly bioactive platelet microparticles and release pro-inflammatory and pro-thrombotic mediators, which interact with each other and activate immune cells [15]. In CTEPH, platelet overactivation [16] and dysfunction [17] have been observed, with platelets adhering to immune cells such as monocytes and

neutrophils, forming aggregates that are elevated in circulation [18]. Despite these observations, their precise contribution to CTEPH and the underlying mechanisms remain unclear. In addition, loss of transforming growth factor  $\beta 1$  (TGFB1) in platelets was associated with venous thrombus resolution [13]. All of the above indicate the interaction between platelets and various blood components in the inflammation and thrombus resolution of CTEPH.

To gain a deeper understanding of platelet-related mechanisms in CTEPH, we turn to platelet-rich plasma (PRP). PRP, a product of autologous blood with a high platelet concentration and a small amount of white blood cells [19, 20], has been a valuable resource for platelet function [21, 22] and the interactions between platelets and other blood components [23]. However, to more accurately focus on platelet-specific proteins and minimize the influence of plasma proteins, we developed a novel approach. After isolating PRP, we centrifuged it to remove the plasma and then froze the resulting plateletrich pellet, which we term the "enriched platelet pellet (EPP)". Analysis of platelet-specific mechanisms may be hampered by the presence of white blood cells and plasma proteins in conventional PRP. Gradient centrifugation is used by EPP to remove plasma, but platelets and their secretory granules are retained, soluble protein interference is lessened, and platelet function is more precisely reflected.

Proteomics is a technique that is widely used in studying cardiovascular diseases (CVD) [24-27], offering valuable insights into disease mechanisms. Since platelets are enucleated cells, megakaryocytes primarily produce their proteins, which are then stored in granules. Consequently, the production of megakaryocytes and the release of platelets following activation are reflected in the protein levels inside platelets [28, 29]. By identifying and quantifying differentially expressed proteins in the EPP from CTEPH patients, we aim to uncover the underlying mechanisms of how platelets contribute to thrombotic persistence and vascular remodeling in CTEPH. Our study focuses on clarifying the protein level variations in this sample type, exploring their relationships with platelet activity, immunoinflammatory responses, and disease severity. The discovery of these key proteins could not only deepen our understanding of the molecular basis of CTEPH but also potentially reveal new treatment targets, offering hope for improved management of this challenging disease.

### **Methods**

### **Human subjects**

This study prospectively enrolled CTEPH patients from the Department of Pulmonary and Critical Care

Medicine at China-Japan Friendship Hospital and healthy individuals from age and sex matched healthy people during the same period. The initial cohort for proteomic analysis included five healthy subjects and seven CTEPH patients. For flow cytometry, as well as plasma and platelet protein detection, a validation cohort composed of 26 CTEPH patients and 20 healthy controls was enrolled. CTEPH was diagnosed through right heart catheterization, in accordance with the 2022 European Pulmonary Hypertension Guidelines [1]. The diagnostic criteria for CTEPH included: (1) effective anticoagulant therapy for at least three months; (2) mean pulmonary artery pressure (mPAP) > 20 mmHg, and pulmonary artery wedge pressure (PAWP) ≤ 15 mmHg; (3) lung scan perfusion defects suggest the presence of perfusion defects, distributed across multiple lobes and/or segments of the lung that do not match pulmonary ventilation. CT pulmonary angiography or pulmonary angiography showed signs of chronic pulmonary thromboembolism, such as annular stenosis, webbing/slit, and chronic complete occlusion (cystic or conical lesions). Patients with newly detected thrombus were excluded from the study. To rule out its impact on platelet function, prostaglandins were not administered to any of the CTEPH patients who were included. Detailed information on the study subjects is provided in Table 1.

### Isolation of enriched platelet pellet from human blood samples

The blood samples anticoagulated with 10% sodium citrate were separated to obtain PRP at room temperature within 4 h after collection. PRP was isolated by adding 5 ml of sodium citrate anticoagulant to 5 ml of platelet separation solution (TBD, PLA2014TBD). Following gradient centrifugation at 280 g for 15 min, the upper layer was extracted to obtain PRP. EPP are obtained by centrifugation at 500 g for 20 min, resuspended with the washing solution, and then centrifuge again. EPP was stored at  $-80\,^{\circ}\text{C}$  until proteomic analysis. Platelet-poor plasma (PPP) was separated by centrifuging a second blood sample at 3000 rpm for 10 min.

### Protein extraction and purification

Proteins were extracted by adding a protein lysis buffer, followed by a 5-min ultrasound on ice. After centrifuging the material for 10 min at 4 °C and 15,000 g, the supernatant was gathered. The Bicinchoninic Acid (BCA) technique was used to determine the protein concentration. Protein solutions were alkylated with 50 mM iodoacetamide for 15 min in the dark after being treated with 8 M urea and reduced for 45 min

**Table 1** Clinical characteristics of the enrolled population in this study

Variables	Discovery cohort			Validation cohort		
	Control	СТЕРН	р	Control	СТЕРН	р
N	5	7		20	26	
Age, year	59.40 ± 3.78	59.86 ± 7.10	0.899	58.80 ± 11.85	60.04±11.31	0.722
Female (%)	3 (60.00)	4 (57.14)	1	11 (55.00)	15 (57.69)	0.54
BMI	$22.57 \pm 3.70$	24.36±6.21	0.58	24.17±5.27	24.46±5.08	0.853
Comorbidity	22.37 = 3.7 0	2 1.30 2 0.2 1	0.50	2, _3.2,	2 10 _ 3.00	0.000
History of VTE, n	0	7		0	24	
Pulmonary disease, n	0	4		0	10	
Chronic heart disease, n	0	3		0	15	
Cancer, n	0	0		0	3	
	0	0		0	4	
Coronary artery disease, n						
Diabetes mellitus, n	0	1		0	3	
Renal Insufficiency, n	0	1		0	4	
Any comorbidities, n	0	7		0	26	
Symptom						
Hemoptysis, n	_	2		_	5	
Dyspnea, n	-	7		=	26	
Thoracodynia, n	-	0		-	2	
Cough, n	_	2		_	9	
Swoon, n	_	2		_	3	
6MWD, m	_	$425.00 \pm 75.00$		-	342.26 ± 89.14	
WHO functional class I/II/III/IV,n	_	0/5/1/1		_	2/15/6/3	
Hemodynamics						
mRAP, mmHg	=	$5.43 \pm 2.82$		=	5.84 ± 3.05	
mRVP, mmHg	_	32.00 ± 7.85		_	28.28 ± 8.47	
mPAP, mmHg	_	49.29 ± 10.81		_	42.28 ± 11.03	
PAWP, mmHg	_	11.14±2.67		_	11.29 ± 2.94	
PVR, dyn·s·cm <sup>-5</sup>	_	1304.64±877.30		_	888.20 (456.69, 1275.45)	
Qp/QS	_	$0.92 \pm 0.20$		_	0.88 (0.86, 0.94)	
CI, L/min/m <sup>2</sup>	_	1.81 (1.80, 1.99)		_	1.87 (1.69, 2.60)	
SvO <sub>2</sub> -IVC, %	_	$72.67 \pm 7.56$		_	72.70 (68.40, 78.20)	
Complete blood count		72.07 ± 7.50			72.70 (00.40, 70.20)	
Platelet count, × 10 <sup>9</sup> /L		166.06 + 56.06			101.00 + 42.52	
	_	166.86 ± 56.06		-	191.88±43.53	
Platelet distribution width, fL	_	12.45 ± 1.13		-	11.79 ± 1.56	
Mean platelet volume, fL	_	10.82±0.79		_	10.45 ± 0.73	
Large platelet ratio, %	_	31.23 ± 5.83		_	28.26 ± 5.82	
Platelet accumulation, %	=	$0.20 \pm 0.05$		=	$0.20 \pm 0.03$	
Laboratory					,	
NT-proBNP, pg/ml	_	504 (222, 2088)		-	504 (99, 1549)	
Urea, mmol/ml	_	$6.49 \pm 2.07$		_	6.64 (4.98, 8.55)	
Uric acid, umol/ml	_	$387.43 \pm 143.42$		_	370.00 (294.00, 435.00)	
Echocardiography						
EPSPAP, mmHg	_	$93.00 \pm 20.62$		-	$78.44 \pm 22.47$	
TAPSE, mm	-	$17.87 \pm 3.76$		-	$17.10 \pm 3.23$	
TAPSE/sPAP	_	$0.18 \pm 0.05$		_	$0.24 \pm 0.10$	
LVEF, %	_	$67.57 \pm 5.41$		_	$68.08 \pm 4.01$	
Drugs						
Anticoagulants						
Warfarin, n	_	0		_	3	
Low molecular weight heparin, n	_	1		_	1	
DOAC, n	_	7		=	24	
Lipid-lowering drug, n	_	2		_	8	
Beta-receptor blockers, n	_	0		_	2	

Table 1 (continued)

Variables	Discovery cohort			Validation cohort		
	Control	СТЕРН	р	Control	СТЕРН	р
Targeted drugs						
Monotherapy (Riociguat), n	-	3		-	21	
Combination therapy, n	_	4		_	5	

CTEPH, chronic thromboembolic pulmonary hypertension; BMI, body mass index; VTE, venous thromboembolism; 6MWD, 6-min walking distance; WHO, World Health Organization; mPAP, mean right atrial pressure; mRAP, mean right atrial pressure; pressure from tricuspid regurgitation; TAPSE, tricuspid annular plane systolic excursion; LVEF, left ventricular ejection fraction; DOAC, direct oral anticoagulants

at 37 °C. After precipitation with pre-cooled acetone, proteins were digested overnight with trypsin and desalted on a C18 column.

#### LC-MS/MS detection

A NanoElute ultra-high performance liquid chromatography (UHPLC) system was used to separate the samples at a flow rate of 300 nl/min. Mobile phases A (0.1% formic acid) and B (0.1% ethyl formate) were employed in a gradient fashion. Samples separated by chromatography were examined using the datadependent acquisition-Parallel Accumulation-Serial Fragmentation (ddaPASEF) mode on a timsTOF Pro2 mass spectrometer. Every sample was allocated to a test batch at random. Three technical repeats were performed on each sample. Data-independent acquisition-neural network (DIA-NN) software was used to standardize the data, and the false discovery rate (FDR) < 1% was used to control the false positive rate. Data acquisition settings included 4 tandem mass spectrometry scans, ion target strength of 10,000, and a dynamic exclusion time of 0.4 min. Specific collision energies and collection windows were adjusted based on ion mobility for optimal mass spectrometric data acquisition.

### Proteomic data quality control

We used DIA-NN (v1.8.1) for the data-independent acquisition analysis. Based on deep learning spectrograms, we chose the options "MBR" to generate a spectrum library from DIA data, and we used this spectrum library to reanalyze DIA data for protein quantification: the FDR of both precursor ions and protein levels is filtered at 1%, and the filtered data can be used for subsequent biogenic analysis.

### Differential protein level analysis

After standardized treatment, quantitative data of protein is required. To identify differentially expressed proteins between the CTEPH and control groups, proteins with fold change  $\geq 1.50$  and p value < 0.05 by t-test were defined as upregulated; proteins with fold

change  $\leq$  0.67 and p value < 0.05 by t-test were defined as downregulated.

### **Functional enrichment analysis**

We used the Kyoto Encyclopedia of Genes and Genomes (KEGG) pathway enrichment analysis to comprehend the functional characteristics of various proteins.

### Protein-protein interaction network

The STRING database (https://cn.string-db.org/) was used in this investigation to contribute differential proteins for the protein–protein interaction (PPI) network. The 'High Confidence' setting (interaction score ≥ 0.700) was used to create the PPI network. The network was then exported in Cytoscape-compatible format for further visualization and refinement.

### **Enzyme-linked immunosorbent assays**

Key proteins were identified based on three criteria: (1) differential level between CTEPH patients and controls; (2) KEGG-enriched function associated with the development of neutrophil extracellular traps (NETs); and (3) possible clinical or functional significance in CTEPH found through literature search. Candidate proteins, including HMGB1 (JONLNBIO, JL-47571, China), cathepsin G (JONLNBIO, JL-15513, China), NOX2 (JONLNBIO, JL-18618, China), ITGB2 (JONLNBIO, JL-53194, China), and PADI4(PAD4) (JONLNBIO, Cat. JL-14597, China), were further validated using sandwich ELISA kits (Cusabio or J&I Biological) according to manufacturers' instructions, using EPP of healthy people and CTEPH patients. P-selectin was tested using PPP from healthy controls and CTEPH patients (Cat.CSB-E04708h, Cusabio, China). A Spark multipurpose plate reader was used to detect absorbance at 450 nm (TECAN).

### Myeloperoxidase-DNA complex detection

As previously described [30], A 1:2000 dilution of an anti-myeloperoxidase (MPO) monoclonal antibody (Biodragon, BD-PE0170) was prepared as a trapping antibody and placed onto a 96-well plate, which was then left overnight at 4 °C. In accordance with the manufacturer's instructions, patient PPP was added to each well

following blocking with 1% bovine serum albumin (BSA) and peroxidase-labeled anti-DNA monoclonal antibody (Roche, Cat. No:11774425001). Following two hours of room temperature incubation, 200  $\mu$ l of phosphate buffer saline (PBS) was added to each well three times, and then peroxidase substrate (ABTS) was added. The absorbance at 405 nm was measured using a Spark° multipurpose plate reader (TECAN) following a 40-min incubation

(2025) 23:1074

### Transmission electron microscopy

Sun et al. Journal of Translational Medicine

For ultrastructural analysis, EPP samples were adhered to slide coated with poly-L-lysine and fixed in 2.5% glutaraldehyde PBS. The sample was then rinsed with 2% osmium tetroxide, fixed, rinsed again, and dehydrated with acetone concentration series (50%, 70%, 90%, 100%) and embedded. A side-mounted Advantage HR CCD camera (Advanced Microscopy Technology) was used to take digital pictures of the thin slices after they had been reverse-dyed (i.e., stained with uranoyl acetate and lead citrate) and examined under a JEOL JEM-1011 electron microscope.

### Flow cytometry

period at 37 °C.

To measure platelet activation, whole blood was diluted with 1:50 platelets labeled with PBS and APC-conjugated anti-human CD41 antibody (BioLegend, Cat.No: 303710) and PE-conjugated anti-human CD62P antibody (Proteintech, Cat.No: 65173-1-Ig). To measure platelet-neutrophil aggregates (PNAs), whole blood was diluted 1:10 with PBS, and platelets were labeled with BV605-conjugated anti-human CD41 (BioLegend, Cat.No:303742). Neutrophils were labeled with APC anti-human CD66b antibody (Biolegend, Cat.No: 396906) and PEcy7 antihuman CD16 (Biolegend, Cat.No: 317339) at 37 °C for 15 min. We measured the relative content of platelet-neutrophil aggregates and the percentage of CD41-positive neutrophils in peripheral blood. Before being re-suspended in PBS for analysis, the samples were centrifuged at 450×g for 5 min after being treated for 15 min with red blood cell lysis buffer (eBioscience, Cat.No: 00-4300-54). A Becton-Dickinson CytoFlex flow cytometer was used to measure and fix the samples. FlowJo software was then used to examine the collected data. To maintain objectivity, two researchers blindly examined the flow cytometry data.

### Immunofluorescence

Immunofluorescence was performed according to previously published methods [31, 32] using rabbit anti-CD41 antibodies (Proteintech, Cat.No: 24552-1-AP), rabbit

anti-MPO antibodies (Abcam, Cat.No: ab208670), and rabbit anti-citrullinated histone H3 (citH3) antibodies (Abcam, Cat.No: ab5103). Before imaging, sections were thoroughly cleaned after being incubated in PBS with 1% BSA for the entire night, incubated in primary antibody for two hours, and then treated with the proper secondary antibody for an hour (SeraCare, 5220-0362, 5220-0336, 5220-0341). CD41<sup>+</sup> is stained red, CitH3 is stained green, and MPO is stained purple. Fluorescent images were scanned by a whole-slide scanning system (Pannoramic SCAN) and then viewed and analyzed with 3DHISTECH CaseViewer software. Consecutive sections were selected for immunofluorescence.

### Movat's staining

After paraffin sections of PEA tissues were dewaxed and dehydrated, basic fuchsin staining solution was prepared. The tissue was sectioned and stained with Harris hematoxylin. Subsequently, the sections were heated in hot water to enhance dye binding to interstitial cells. After staining, nuclei and elastic fibers appeared black, collagen and reticular fibers yellow, proteoglycan blue-green, and cellulosic materials dark red.

### Statistical analysis

Statistical analyses were performed using PRISM 7.0 (GraphPad) and SPSS 25 software. The FDR was applied to control for multiple statistical testing. Data are presented as mean ± standard error. Statistical significance was evaluated using the t-test. Flow cytometry data were analyzed in a blinded manner by two independent researchers. The data's normality was confirmed using suitable statistical evaluations, like the Shapiro-Wilk test, before any further analysis were carried out. The relationships between the flow cytometry-derived indices and the hemodynamic and right-heart function parameters were assessed using Pearson's or Spearman's correlation coefficient. The diagnostic performance of particular biomarkers was assessed using receiver operating characteristic (ROC) curve analysis. Statistical significance was defined as a *p*-value of less than 0.05.

### **Results**

### Enriched platelet pellet isolation and quantitative proteomic analysis

The workflow for enriched platelet pellet isolation and subsequent proteomic analysis is depicted in Fig. 1A. The distribution and quantity of detected peptides for each protein are presented in Fig. 1B and C, offering a detailed overview of the platelet proteome in patients with CTEPH. A total of 5554 proteins were identified in

Sun et al. Journal of Translational Medicine (2025) 23:1074 Page 7 of 17

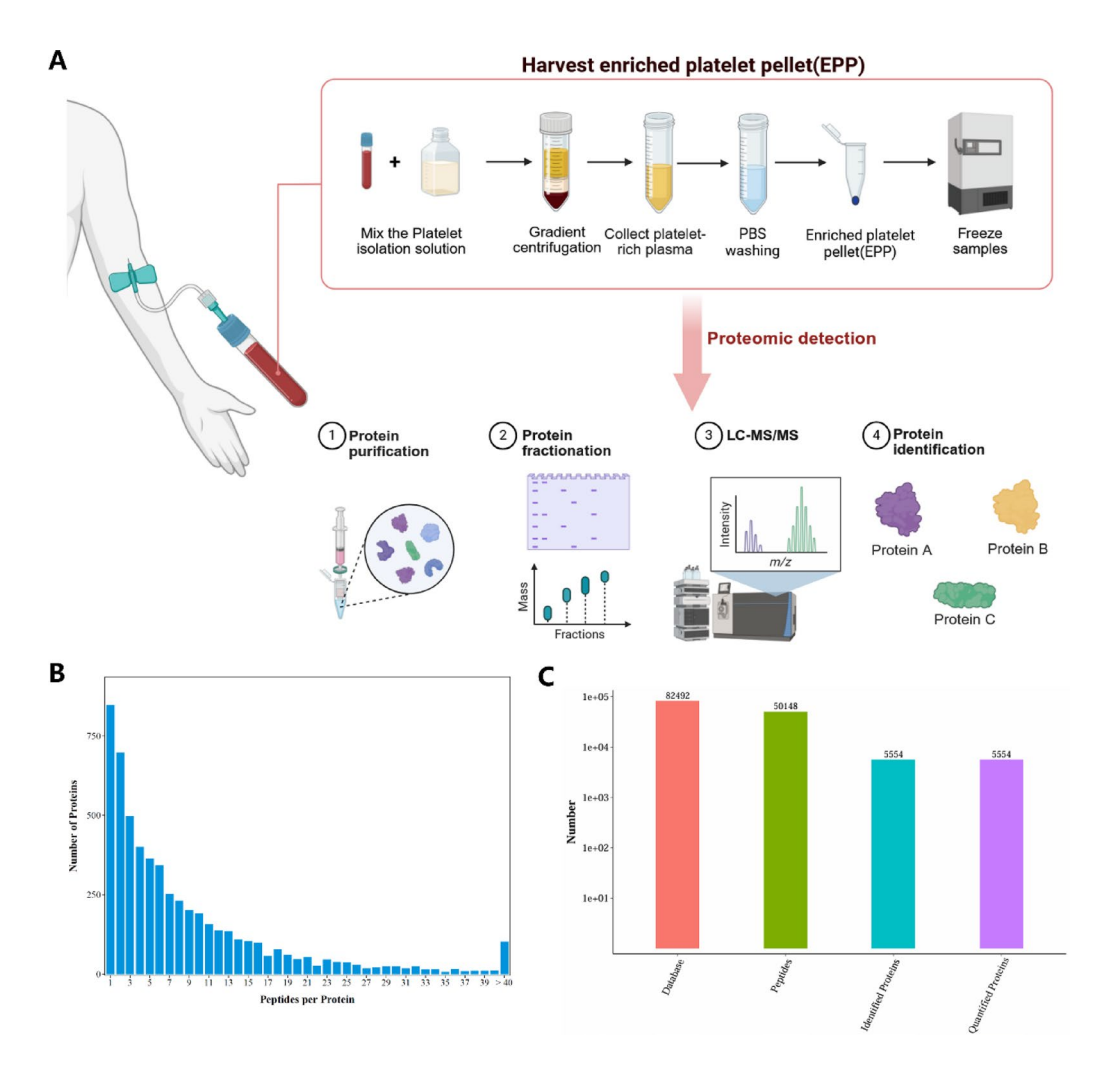


**Fig. 1** Enriched-platelet pellet isolation, extraction, and proteomic analysis. **A** Schematic diagram shows the process of obtaining human platelet-rich plasma from peripheral blood and collecting enriched-platelet pellet (EPP) for proteomic detection. **B** The distribution of the number of peptides detected per protein in the total protein content of EPP. The horizontal axis represents the number of peptide segments, and the vertical axis represents the number of proteins corresponding to the peptide segments. **C** Bar graph shows the number of identified and quantified proteins detected

proteomic analysis, and 5554 of them contained quantitative information (Fig. 1C).

### Differentially expressed proteins and enriched pathways in CTEPH

To explore alterations in EPP proteome in CTEPH, we first analyzed differential proteins using bioinformatics methods. As shown in Fig. 2A, the EPP proteome of CTEPH patients exhibited distinct biological characteristics compared to healthy controls. It was discovered that the level of 179 proteins varied considerably, with 111 showing an increase and 68 showing a decrease (Fig. 2B and D). The heatmap illustrates the differences in level between the top 10 upregulated and downregulated proteins (Fig. 2C), showing clear distinction between CTEPH and healthy controls. The enriched KEGG

pathways in CTEPH (Figs. 2E) were mainly concentrated in coagulation and complement activation, phagosome and NET formation (Figs. 2E). The PPI network of the differential proteins is shown in Fig. 2F, suggested that PADI4, CYBB, CTSG and other proteins are key proteins in EPP and may be involved in disease progression.

### Validation of differential proteins of the neutrophil extracellular trap pathway

PADI4, NOX2, HMGB1, CTSG and ITGB2 identified in the KEGG pathway enrichment analysis were found to partially overlap with proteins associated with the phagosome and NET formation pathways. It was also reported that NET promote thrombus fibrosis in CTEPH [33]. To validate our proteomic results, we performed ELISA assays for proteins associated with NET formation. In

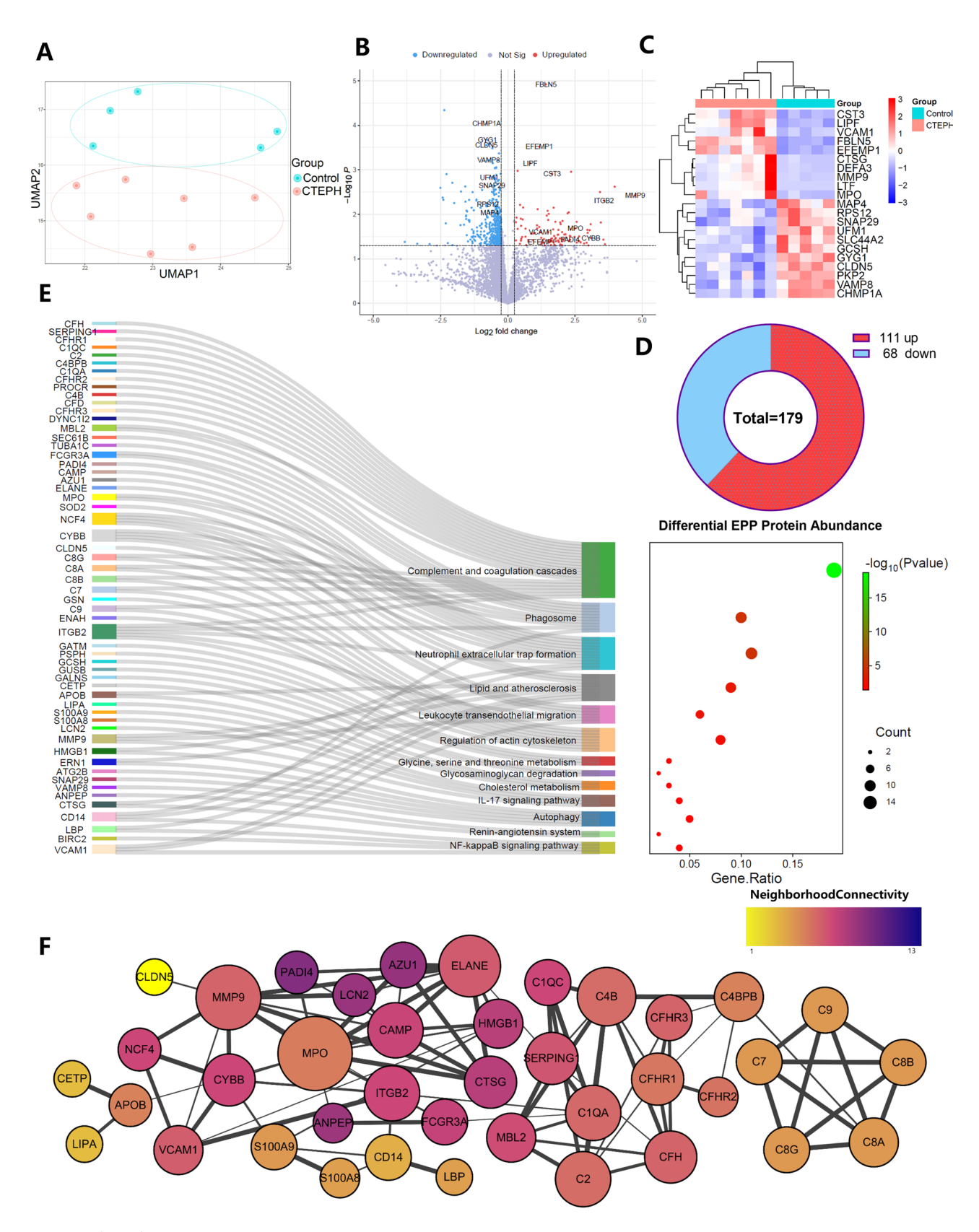


Fig. 2 (See legend on next page.)

(See figure on previous page.)

**Fig. 2** Differential proteins in EPP proteome and functional enrichment analyses. **A** Uniform Manifold Approximation and Projection (UMAP) displays an ellipse plot possibly showing clustering or principal component. **B** Volcano plot visualizes differential protein level with log fold change on the x-axis and negative log of the p-value on the y-axis. Proteins that are significantly upregulated are shown in red, downregulated in blue, and non-significant in grey. **C** Heatmap represents the level levels of the top 10 differential proteins between CTEPH and healthy controls, with higher level in red and lower level in blue. **D** Figure represents the number of differentially expressed proteins in CTEPH. **E**The top 10 enrichment KEGG pathways ranked by enrichment score. **F** PPI network of differential proteins. Nodes represent differentially expressed proteins colored by neighborhood connectivity

the validation cohort, CTEPH patients had significantly higher levels of NOX2 (p<0.0001), PAD4 (p<0.0001), ITGB2 (p=0.0228), cathepsin G (CTSG) (p<0.0001), and HMGB1 (p=0.0005) (Fig. 3A–E) than healthy controls. In addition, ROC curve showed that NOX2 (AUC=0.956), PAD4 (AUC=0.989), CTSG (AUC=0.911) had relatively high diagnostic efficiency (Fig. 3F). Therefore, the high diagnostic efficiency of NOX2, PAD4 and CTSG means that these proteins may be key nodes in the pathogenesis of CTEPH, providing potential biomarkers for the early diagnosis of CTEPH.

### Correlation between candidate protein levels and clinical parameters of CTEPH

NOX2 exhibited a positive correlation with the estimated pulmonary artery pressure from tricuspid regurgitation (EPSPAP) ( $r=0.485,\ p=0.03$ ) and a significant correlation with total pulmonary resistance (TPR) ( $r=0.608,\ p=0.007$ ). Notably, PAD4 levels exhibited significant correlation with EPSPAP ( $r=0.594,\ p=0.006$ ), TPR ( $r=0.681,\ p=0.002$ ), and D-dimer ( $r=0.568,\ p=0.009$ ). Furthermore, there was a negative association between PAD4 levels and tricuspid annular plane systolic excursion (TAPSE)/EPSPAP ( $r=-0.450,\ p=0.046$ ) and a positive correlation with pulmonary vascular resistance (PVR) ( $r=0.529,\ p=0.024$ ) and inferior vena cava diameter (IVC-d) ( $r=0.516,\ p=0.028$ ). These findings indicated that PAD4 was strongly associated with the severity of CTEPH (Fig. 4).

We subsequently found significant increases in PAD4 levels were observed in patients with a right ventricular transverse diameter/left ventricular transverse diameter (RV/LV) ratio≥1.27 (mild dilatation of the right heart [34]) (p = 0.035), inferior vena cava collapse index (IVC-CI) < 50% (abnormal collapse of the inferior vena cava caused by right heart failure [35])(p = 0.011), and pericardial effusion (p = 0.008) (Table 2). TAPSE/ EPSPAP is a common indicator for predicting deterioration of right heart function in PH [35]. The best cut-off value for the TAPSE/sPAP ratio for predicting mortality was 0.20 mm/ mmHg [36]. When we used 0.20 mm/mmHg as the threshold, patients with lower TAPSE/sPAP ratio (< 0.20) had significantly higher NOX2 and PAD4 levels (Table 3), indicating that the levels of PAD4 reflected the severity of CTEPH and was related to the deterioration of right heart function.

**Table 2** Relationship between PAD4 and indicators of right heart function

Page 9 of 17

neart function		
	PAD4 (ng/mL)	<i>p</i> value
RV/LV		0.035
< 1.27	$13.92 \pm 8.28$	
≥ 1.27	$25.69 \pm 14.54$	
RV-b, mm		0.065
< 50	$15.40 \pm 8.40$	
≥50	$26.30 \pm 16.71$	
EPSPAP, mmHg		0.06
< 75	$14.08 \pm 9.35$	
≥75	$26.95 \pm 13.95$	
TAPSE, mm		0.603
< 16	$20.91 \pm 16.63$	
≥16	$17.83 \pm 8.97$	
IVC-CI		0.011
≥50%	$16.15 \pm 8.81$	
< 50%	$33.88 \pm 17.09$	
Pericardial effusion		0.008
No	$15.13 \pm 8.36$	
Yes	$31.47 \pm 16.45$	

PAD4, peptidylarginine deiminase 4; RV/LV, right ventricular transverse diameter/left ventricular transverse diameter; RV-b, right ventricular basal transverse diameter; EPSPAP, estimated pulmonary artery pressure from tricuspid regurgitation; TAPSE, tricuspid annular plane systolic excursion; IVC-CI, inferior vena cava collapse index

**Table 3** Differences in levels of key proteins between groups based on TAPSE/EPSPAP

Variables	TAPSE/ EPSPAP	P value		
	< 0.20	≥0.20	•	
N	10	15		
PAD4 (ng/ml)	$27.91 \pm 14.75$	14.53 ± 8.87	0.02	
CTSG (ng/ml)	$10.13 \pm 5.97$	$8.43 \pm 3.21$	0.45	
NOX2 (ng/ml)	11.23 (10.27, 12.83)	7.37 (3.61, 9.01)	0.037	
ITGB2 (ng/ml)	1.77 (1.19, 2.35)	2.15 (1.55, 3.02)	0.438	
HMGB1 (pg/ml)	251.48 ± 128.42	375.64 ± 163.66	0.099	

PAD4, peptidylarginine deiminase 4; CTSG, cathepsin G; NOX2, nicotinamide adenine dinucleotide phosphate (NADPH) oxidase 2; ITGB2, integrin beta 2; HMGB1, high mobility group box-1 protein; EPSPAP, estimated pulmonary artery pressure from tricuspid regurgitation; TAPSE, tricuspid annular plane systolic excursion

### Increased platelet activation and P-selectin release in CTEPH

To explore the changes in platelet function, we measured platelet activation and plasma P-selectin levels in CTEPH patients. Flow cytometry showed increased platelet P-selectin

Sun et al. Journal of Translational Medicine (2025) 23:1074 Page 10 of 17

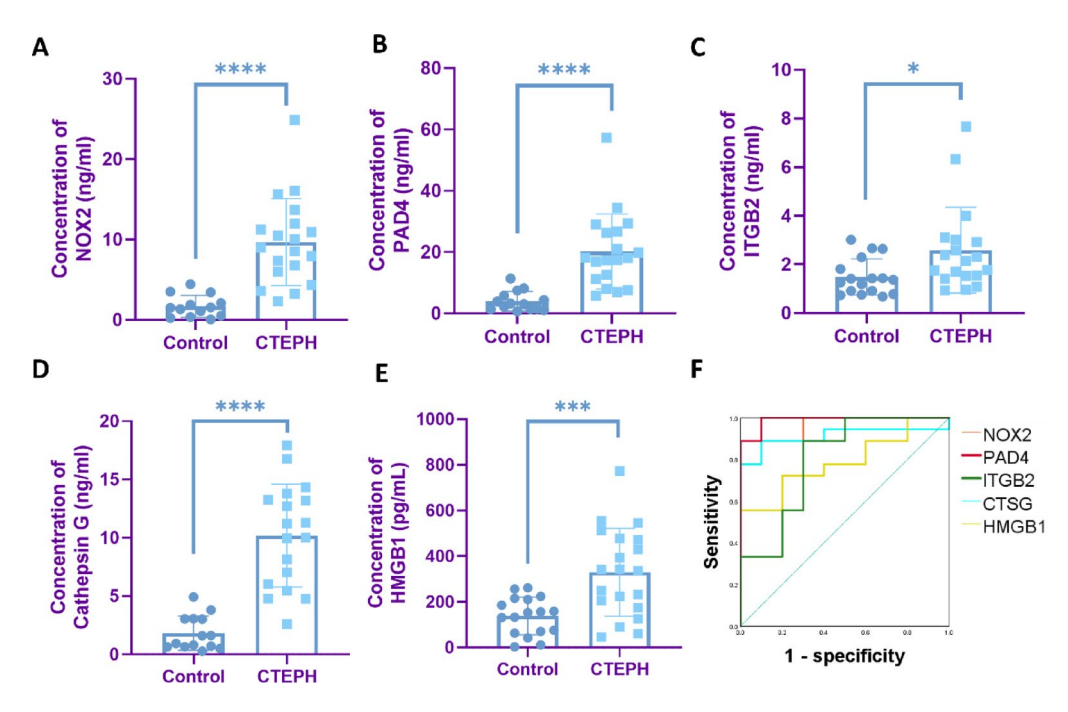


**Fig. 3** Verification of differentially expressed proteins in validation cohort. **A–E** Concentration of **A** NOX2, **B** PAD4, **C** ITGB2, **D** Cathepsin G, and **E** HMGB1 in enriched-platelet pellet (EPP) of healthy controls and CTEPH patients were measured by ELISA. **F** Receiver operating characteristic (ROC) results of the candidate proteins between CTEPH and healthy controls. Statistical significance was determined by Student's t-test. \* *p* value < 0.005; \*\*\*\* *p* value < 0.001; \*\*\*\* *p* value < 0.0001

expression (p<0.0001) (Fig. 5A and B) and increased plasma soluble P-selectin level (p=0.008) in CTEPH patients (Fig. 5C). Transmission electron microscope analysis showed that platelets of CTEPH patients extended pseudopodia, releasing the platelet-derived particles in the form of exocytosis (Fig. 5D). These studies suggest that platelet activation of CTEPH is increased and that the release of platelet-derived particles may be involved in disease progression .

### Platelet-neutrophil interactions and NET formation in CTEPH

To investigate the potential interactions between platelet activation and neutrophils, we first used flow cytometry to detect the proportion of PNAs (Fig. 6A). PNAs were significantly increased in CTEPH compared to controls (Fig. 6B). Next, we examined relative level of MPO-DNA complex, a key marker of NET formation, and found a similarly significant increase in CTEPH patients compared to controls (Fig. 6C). Moreover, relative level of MPO-DNA complex was positively correlated with the concentration of ITGB2 in EPP (r = 0.875, p < 0.0001) (Fig. 6D) and plasma P-selectin concentration (r = 0.477, p = 0.045) (Fig. 4E). Additionally, we performed immunofluorescence and Movat's staining on the same tissue sections from PEA tissues to examine the role of NET formation in thrombus resolution (Fig. 6F). During the early thrombolysis stage, within the area of fresh thrombi, there was predominantly a large amount of co-localization of CD41 and MPO, along with a small amount of co-localization of CD41, MPO, and CitH3. In the thrombus fibrosis stage, a substantial number of co-localizations of CD41, MPO, and CitH3 were observed in the chronic thrombus region, dispersed within the MPO-positive components. At the neointima formation stage, a small amount of co-localization of CD41, MPO, and CitH3 was scattered among the neointima (Fig. 6F). These findings indicate that platelet-neutrophil interactions are closely associated with NET formation, and the presence of NETs may influence delayed thrombus resolution and contribute to the progression of CTEPH.

### **Discussion**

This study, for the first time, combines enriched platelet pellet (EPP) proteomic analysis with experimental approaches such as flow cytometry and electron microscopy to provide a multidimensional view of platelet activity in CTEPH. We identified significant differences in the EPP proteome between healthy individuals and CTEPH patients, suggesting that platelets are essential to the etiology of the illness. Important proteins, such as NOX2 and PAD4, were discovered to be strongly correlated with the severity of the disease and the function of the right heart, indicating that they may be used as therapeutic targets and biomarkers for the advancement of CTEPH.

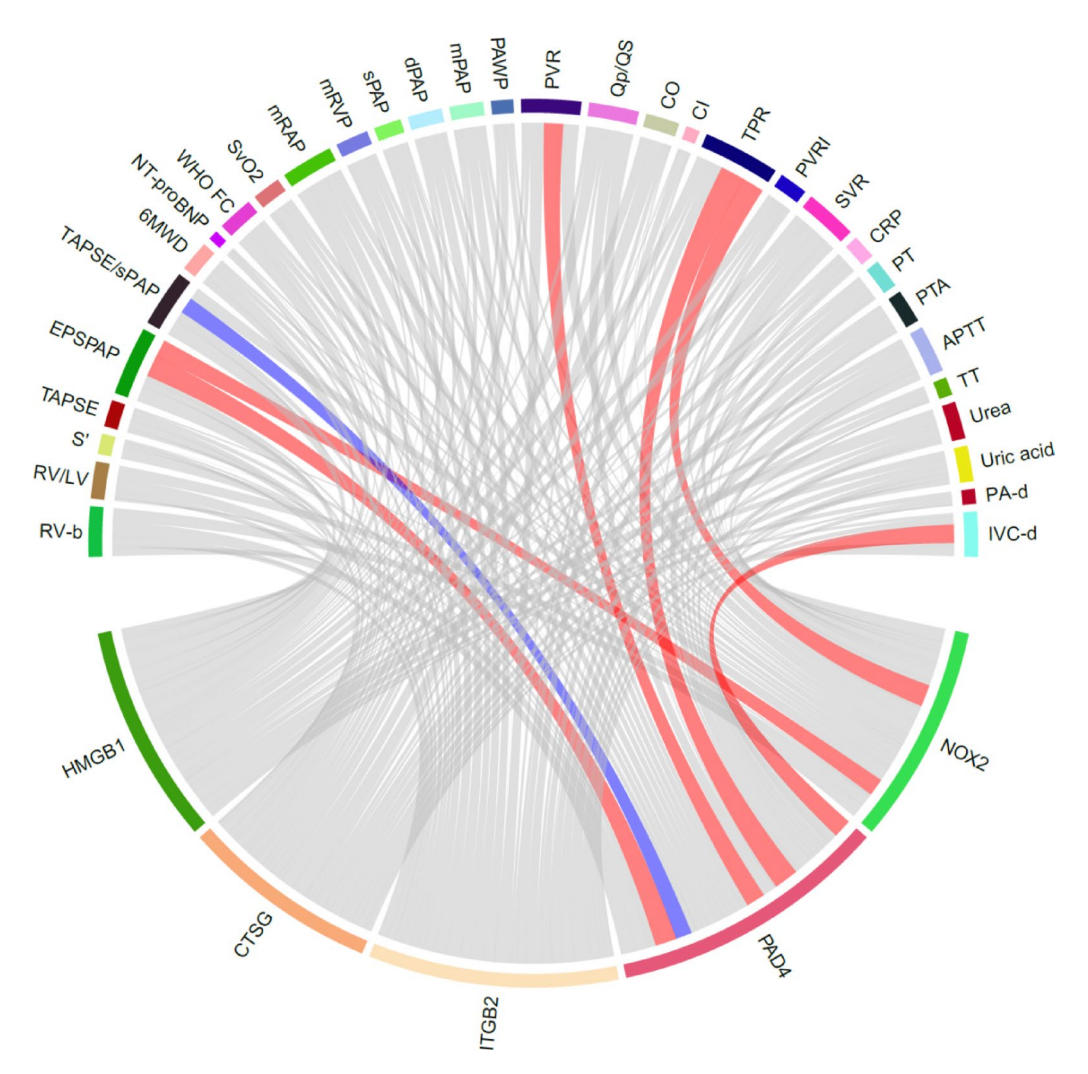


**Fig. 4** Analysis of the correlation between differentially expressed proteins and clinical parameters in the validation cohort. Correlations with statistical significance (*p* value < 0.05) are indicated in red for positive correlations and in blue for negative correlations. Non-significant correlations (*p* value > 0.05) are indicated in gray. *Abbreviations*: PAD4, peptidylarginine deiminase 4; CTSG, cathepsin G; NOX2, nicotinamide adenine dinucleotide phosphate (NADPH) oxidase 2; ITGB2, integrin beta 2; HMGB1, high mobility group box-1 protein; 6MWD, 6-min walking distance; WHO FC, World Health Organization Functional Class; NT-proBNP, N-terminal pro-brain natriuretic peptide; mPAP, mean pulmonary artery pressure; PVR, pulmonary vascular resistance; CO, cardiac output; Cl, cardiac index; SvO<sub>2</sub>, mixed venous oxygen saturation; sPAP, pulmonary artery systolic pressure; dPAP, pulmonary artery diastolic pressure; sRAP, right atrial systolic pressure; PAWP, pulmonary artery wedge pressure; Qp/Qs, pulmonary-to-systemic blood flow ratio; TPR, total pulmonary resistance; PVRI, pulmonary vascular resistance index; SVR, systemic vascular resistance; CRP, C-reactive protein; PT, prothrombin time; PTA, prothrombin activity; APTT, activated partial thromboplastin time; RV-b, right ventricular basal diameter; RV/LV, the right ventricular to left ventricular ratio; S′, tricuspid lateral annular longitudinal systolic velocity; TAPSE, tricuspid annular plane systolic excursion; EPSPAP, estimated pulmonary artery pressure from tricuspid regurgitation; PA-d, pulmonary artery diameter; IVC-d, inferior vena cava diameter

Moreover, platelet-neutrophil interactions and NET formation may contribute to a delay in thrombus resolution, advancing our understanding of CTEPH mechanisms and highlighting new therapeutic directions.

Platelets are crucial in hemostasis and thrombosis, and alterations in platelet protein levels can lead to dysfunctions such as platelet adhesion and release, contributing to the development of CVDs [37, 38]. PRP proteomic analyses focus on the comprehensive analysis of proteins,

growth factors, cytokines, and other bioactive molecules within PRP samples [39], providing valuable insights into the molecular mechanisms involved in tissue repair [39], angiogenesis [40], inflammation resolution [41], and immune modulation [42]. Traditional PRP contains platelets, plasma proteins, and leukocytes, complicating the interpretation of platelet-specific mechanisms due to potential interference. In this study, we analyzed the proteome of "enriched platelet pellet"—prepared

Sun et al. Journal of Translational Medicine (2025) 23:1074 Page 12 of 17

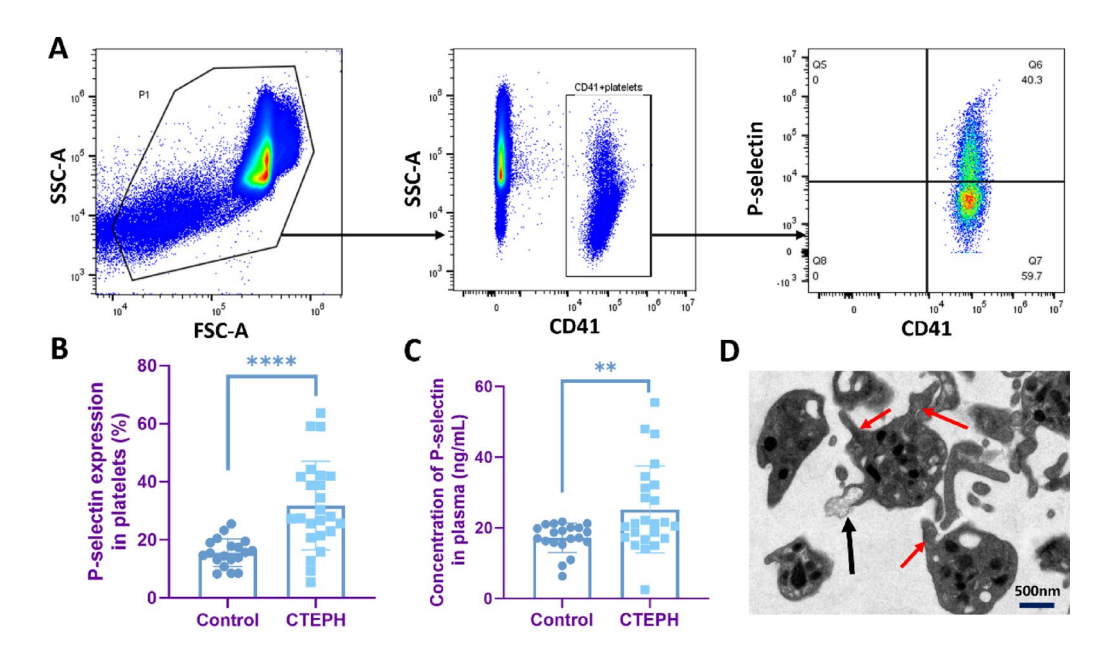


**Fig. 5** Level of platelet P-selectin and platelet morphology. **A** The plot depicts the gating strategy used to identify platelet populations. The defined region indicates the platelet population determined by size and complexity characteristics measured via flow cytometry. Platelet activation is evaluated by the percentage of CD41\* platelets that are also positive for P-selectin. **B** and **C** Expression levels of P-selectin in platelets (**B**) and its concentration in plasma (**D**) in healthy individuals and CTEPH patients. **D** Transmission electron microscopy (TEM) was employed to visualize the ultrastructure of platelets from a non-stimulated sample from CTEPH patients, specifically revealing the presence of dense granules. As shown in the TEM images, black arrows indicate the platelet-derived particles released by platelets, while red arrows point to the pseudopodia extended by activated platelets. Scale bars, 500 nm. Statistical significance was determined by Student's t-test. \*\* p value < 0.001; \*\*\*\* p value < 0.0001

by centrifuging PRP to remove most plasma and preserve platelet-enriched precipitates—to balance physiological relevance and proteomic specificity. This method reduces soluble plasma protein and leukocyte-derived protein interference while retaining platelet-derived microparticles and surface receptors. This study concurrently measured the plasma P-selectin level to remove plasma interference, and it was shown to be consistent with platelet P-selectin expression, further establishing that platelet activation was the primary driving element. Notably, trace leukocyte-derived proteins may persist due to residual white blood cells in EPP, reflecting the interaction between platelets and immune cells. Moreover, the study's NET-related protein level showed a strong correlation with platelet activation markers (P-selectin), indicating that platelet-neutrophil interactions rather than simple white blood cell contamination were the primary cause.

Although these proteins may not always come from platelets, we found in our study that NET development in EPP was linked to increased levels of HMGB1, PAD4, NOX2, ITGB2, and CTSG. Due to the complexity of the components within EPP, platelets may bind to immune cells in specific forms, such as aggregates. Platelet activation not only leads to the formation of aggregates with immune cells, but also causes high mobility group box-1 protein 1 (HMGB1) to be released, a molecule that can independently promote platelet aggregation [43–45],

activation of neutrophils, and initiation of NET formation [46, 47]. Through Toll-like receptors (TLRs) and receptor for advanced glycation end-products (RAGE), HMGB1 reciprocally activates platelets, promoting platelet activation and the consequent release of regulatory factors that cause pathological thrombosis linked to inflammation [48]. Increased nicotinamide adenine dinucleotide phosphate oxidase 2 (NOX2) enzyme activity in platelets leads to an increase in reactive oxygen species (ROS) [49-51], enhancing the activation of neutrophils and platelets [52]. Activated neutrophils adhere to more platelets, secrete cathepsin G [53] and neutrophil elastase (NE) [54], and further promote platelet activation [55]. Next, ROS stimulates MPO to act synergically with neutrophil elastase [56], initiating chromatin release and the formation of MPO-DNA complex. Peptidylarginine deiminase 4 (PAD4), as an important post-translational modification enzyme, continues to mediate citrullination of chromatin histone proteins [57], which leads to the formation of citH3 [56]. Therefore, the results shown by MPO, citH3 and NE have been recognized as the most reliable markers of NET formation [58, 59]. Given that PAD4 is usually associated with neutrophils [59], the detected signals may represent a complex of activated platelets and neutrophils. Our findings also revealed an increase in NOX2, PAD4, and HMGB1, which may indicate that the process by which platelets contribute to the development of NETs has been activated [59]. Interestingly, the Sun et al. Journal of Translational Medicine (2025) 23:1074 Page 13 of 17

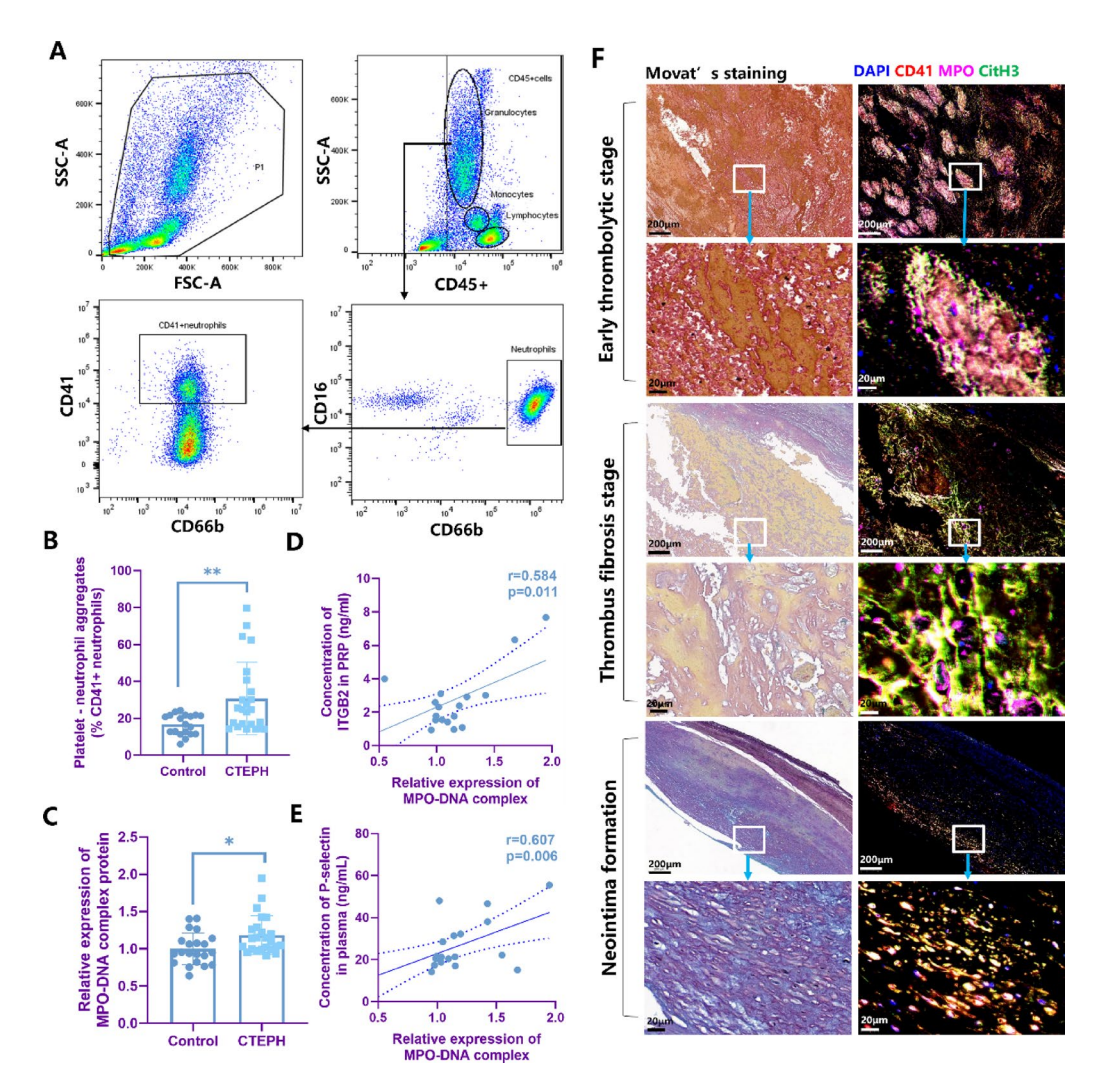


**Fig. 6** Platelet-mediated NET formation and its link to CTEPH thrombus resolution. **A** Flow cytometry demonstrates the identification of different populations of immune cells (granulocytes, monocytes, lymphocytes). Co-level of CD16 and CD66b is defined as neutrophils, and the proportion of CD41-positive groups in neutrophils is analyzed. **B** Quantification of CD41+platelet-neutrophil aggregates in CTEPH patients compared to healthy controls. **C** Quantification of MPO-DNA complex protein in CTEPH patients compared to healthy controls. **D** Correlation between MPO-DNA complex levels and ITGB2 concentration in CTEPH patients. **E** Correlation between MPO-DNA complex levels and P-selectin concentration in CTEPH patients. **F** The left column displays Movat's staining under light microscopy, showing the early thrombus lysis stage, the thrombus fibrosis stage, and the neointima formation stage of CTEPH. The right column displays multiplex immunofluorescence, showing the immunostaining of CD41 (red), MPO (pink), citH3 (green), and nuclear staining (DAPI, blue). CD41, MPO, and citH3 were co-expressed in the early thrombus lysis stage, the thrombus fibrosis stage, and the neointima formation stage. Statistical significance was determined by Student's t-test. \* p value < 0.05; \*\* p value < 0.01

levels of PAD4 and NOX2 are correlated with right heart dysfunction and hemodynamic indicators, indicating an increase in ROS [48]. Under oxidative stress conditions, the formation of NET increases, mediating the organization of thrombus locally. In summary, this cascade of platelet-induced neutrophil activation may be essential for NET development, and NETs can then further activate platelets, generating a positive feedback loop (Fig. 7). NET production can be decreased by inhibiting PAD4. A reduction in PAD4 has been shown to lower thrombosis in mice models [60, 61]. Targeting PAD4 may be a novel tactic to halt the course of CTEPH, according to the study's link between PAD4 and right heart function.

We speculate that inhibiting PAD4 can reduce the production of citrullinated histones in NETs, blocking the thrombus fibrosis signal [59]; at the same time, it can decrease the interaction between platelets and neutrophils [57], breaking the vicious cycle of inflammation and thrombosis. This series of events might contribute to the pathogenesis and progression of CTEPH, potentially explaining the elevated levels of related markers in patients with this disease.

Platelets must first adhere to the injured endothelial surface, become activated. A variety of storage particles, including lysosomes,  $\alpha$  particles, and  $\delta$  particles, are abundant in platelets [62]. These particles include

Sun et al. Journal of Translational Medicine (2025) 23:1074 Page 14 of 17

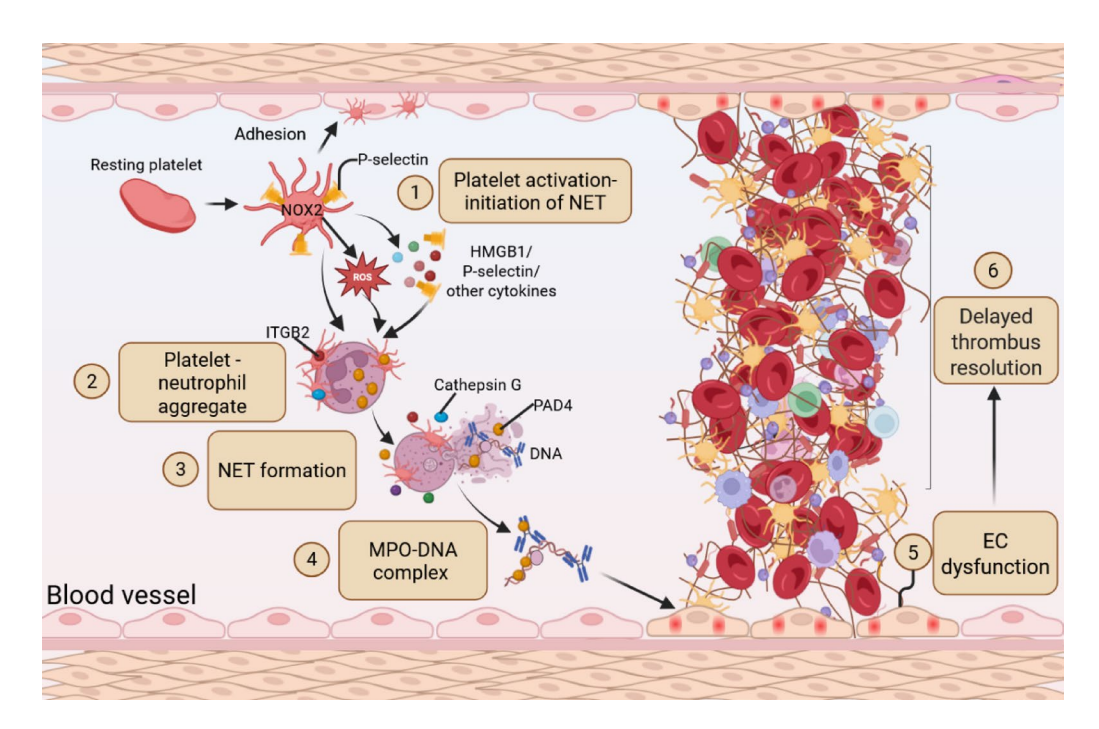


**Fig. 7** The mechanism of platelet involvement in CTEPH. Platelets first adhere to the injured endothelial surface, become activated in response to signals such as P-selectin and other cytokines (e.g., HMGB1), leading to the release of inflammatory molecules. The increase of platelet NOX2 leads to the increase of ROS and promotes the formation of neutrophil extracellular trap (NET). Then the interaction between activated platelets and neutrophils through integrin β2(ITGB2) results in the formation of platelet-neutrophil aggregates. Platelet-neutrophil aggregates release DNA, PAD4, cathepsin G and intracellular substances in the form of NETs. Moreover, under the action of PAD4, the interaction between neutrophil-derived DNA and MPO forms the MPO-DNA complex, further promoting inflammation and coagulation. Activated platelets and the MPO-DNA complex contribute to endothelial dysfunction, which delayed thrombus resolution. *Abbreviations*: NOX2, nicotinamide adenine dinucleotide phosphate (NADPH) oxidase 2; ROS, reactive oxygen species; PAD4, peptidylarginine deiminase 4; MPO, myeloperoxidase; HMGB1, high mobility group box-1 protein; EC, endothelial cell

bioactive chemicals, soluble proteins, and receptors that are essential for immunity, inflammation, and hemostasis [63]. P-selectin is a transmembrane protein stored in  $\alpha$ particles of platelets [64]. P-selectin translocations during platelet activation interact with endothelium and white blood cells' P-selectin glycoprotein ligand-1 (PSGL-1) to mediate the inflammatory process [65]. When blood vessel walls are damaged, platelets get activated, adhere to the damaged site, change their shape, secrete the contents of their granules, and start to form aggregates [66]. P-selectin binding to PSGL1 attracts neutrophils to the site of thrombosis [65]. Integrin  $\beta$ 2 (ITGB2) then strengthens the attachment of neutrophils to platelets by interacting with fibrinogen [67], which is often described as a "vicious cycle" [68](Fig. 7). In this study, the positive correlation between P-selectin and MPO-DNA (r = 0.477) suggests that the formation of PNAs can induce neutrophils to release NETs.

In PEA tissues, the entire process of acute thrombus transformation into insoluble fibrotic vascular obstruction and subsequent vascular remodeling can be observed [11, 12, 69]. While the exact cause of delayed thrombus resolution remains unclear, NETs have been identified as an upstream trigger of TGF- $\beta$ -mediated delayed thrombus resolution. The presence of NETs, coupled with the

overactivity of TGF-β, exacerbates the fibrotic response in venous thrombosis in mice [13]. Based on the mechanism, we hypothesize that DNA and histones released by NETs activate TGF- $\beta$  receptors [13]. PAD4-mediated histone citrullination enhances TGF-β signaling activity [70]. DNA, histones, PAD4 and MPO-DNA complex collectively promote thrombus fibrosis and pulmonary vascular remodeling. In our study, we found that NETs were present throughout the early thrombolytic stage, the thrombus fibrosis stage, and the neointima formation stage, suggesting that NETs may contribute to delayed thrombus resolution. Additionally, NETs were able to transform mononuclear cells from CTEPH patients into fibroblast-like cells [33]. We observed a significant presence of NETs in the neointima region and hypothesize that NETs may promote fibroblast proliferation and transformation, further exacerbating pulmonary vascular remodeling. This may also explain the correlation between these platelet-associated proteins and disease severity.

Although these results provide insightful information, we recognize that the results' generalizability may be constrained by the observational approach and a small sample size. Nonetheless, the ROC curve AUC of important proteins (such PAD4 and NOX2) was greater

than 0.9, indicating that the findings were somewhat reliable. Further large-sample verification at many centers is necessary. Furthermore, difference analysis was not possible since the healthy control group lacked clinical parameters. Whether PAD4 and NOX2 were particular indicators of CTEPH could not be ascertained in this investigation. With an emphasis on their functions in platelet-neutrophil interactions and NET formation in CTEPH, further research should be confirmed in additional subtypes of pulmonary arterial hypertension. Moreover, targeting these aggregates formation potentially reduce NET-mediated thrombus fibrosis and promote more effective thrombolysis. Longitudinal studies are essential to assess dynamic changes in protein level throughout disease progression. Additionally, we have found that patients with CTEPH emit extracellular vesicles originating from platelets. Therefore, to ascertain their function in the course of disease, the intracellular proteins and extracellular vesicles of platelets can be distinguished by subcellular fractionation technology.

### **Conclusion**

In summary, this study underscores the utility of enriched platelet pellet proteomics in elucidating the intricate interactions between platelets, immune cells, and coagulation pathways in CTEPH. This study offers fresh perspectives on the disease mechanism by highlighting the critical roles that PAD4 and NOX2 play in platelet activation and NET formation in CTEPH. These results point to PAD4 as a possible therapeutic target or biomarker and provide fresh insights into the biology of CTEPH. Elevated P-selectin levels further establish a link between platelet activation and thrombo-inflammatory processes. Multi-center large-sample studies are required to confirm its clinical utility as a biomarker and therapeutic target.

### Abbreviations

BSA Bovine serum albumin citH3 Citrullinated histone H3

CTEPH Chronic thromboembolic pulmonary hypertension

CTSG Cathepsin G

CVD Cardiovascular diseases
DVT Deep vein thrombosis
FPSPAP Estimated systolic pulm

EPSPAP Estimated systolic pulmonary artery pressure

HMGB1 High mobility group box-1 protein 1

ITGB2 Integrin β2

IVC-CI Inferior vena cava collapse index IVC-d Inferior vena cava diameter

KEGG Kyoto encyclopedia of genes and genomes

mPAP Mean pulmonary artery pressure

MPO Myeloperoxidase
NE Neutrophil elastase
NET Neutrophil extracellular trap

NOX2 Nicotinamide adenine dinucleotide phosphate oxidase 2

PAD4 Peptidylarginine deiminase 4
PAWP Pulmonary artery wedge pressure

PBS Phosphate buffer saline
PE Pulmonary embolism
PEA Pulmonary endarterectomy

PNA Platelet-neutrophil aggregate PPI Protein-protein interaction

PRP Platelet-rich plasma

PSGL-1 P-selectin-P-selectin glycoprotein ligand-1

PVR Pulmonary vascular resistance
ROS Reactive oxygen species
RV-b RV basal diameter

RV/LV Right ventricular transverse diameter/left ventricular transverse

diameter

TAPSE Tricuspid annular plane systolic offset
TGFB1 Transforming growth factor β1
TPR Total pulmonary resistance

WHO FC World health organization functional classification

#### Acknowledgements

Not applicable.

#### **Author contributions**

Zhenguo Zhai, Peiran Yang, Shiqing Xu and Lu Sun conceive and design the experiments. Lu Sun, Yuhan Li, Han Tian, Shiqing Xu and Min Liu conducted the experiments. Lu Sun and Haobo Li performed the data analysis. Xincheng Li, Han Tian, Zhenguo Zhai, Zhu Zhang, Qiang Huang, and Jixiang Liu provided valuable revision suggestions. Kuangxun Li, Xiaofan Ji, and Mengjie Duo were responsible for research supervision and coordination. Bingzhang Zou, Yunxia Zhang, Shuai Zhang, Wanmu Xie, and Peiran Yang were in charge of research strategic planning. Jinzhi Wang, Jing Wen, Ximei Niu, Linfeng Xi, Yishan Li collected clinical samples. Lu Sun drafted the manuscript. Dingyi Wang, Ran Miao, Peiran Yang, Shiqing Xu and Zhenguo Zhai reviewed and edited the manuscript. All authors read and approved the final manuscript.

#### Funding

This work was supported by the National Natural Science Foundation of China (82241029, 82270062), CAMS Innovation Fund for Medical Sciences(CIFMS)( 2021-I2M-1-061), the National High Level Hospital Clinical Research Funding (2022-NHLHCRF-LX-01-01-02), the National Key Research and Development Program of China (2023YFC2507200), the Chinese Academy of Medical Sciences Innovation Fund for Medical Sciences (2021-I2M-1-001, 2023-I2M-2-001), Non-Profit Central Research Institute Fund of the Chinese Academy of Medical Sciences (2021-RC310-016), and State Key Laboratory Special Fund (2060204).

### Data availability

The data that support the findings of this study are available from the corresponding author upon reasonable request.

### **Declarations**

### Ethics approval and consent to participate

All sample collection procedures were approved by the China-Japan Friendship Hospital ethics committee (2022-KY-085), and written informed consent was obtained from all participants.

### **Competing interests**

The authors declare no competing interests.

### Author details

<sup>1</sup>China-Japan Friendship Hospital, Chinese Academy of Medical Sciences & Peking Union Medical College, Beijing, China

<sup>2</sup>National Center for Respiratory Medicine, State Key Laboratory of Respiratory Health and Multimorbidity, National Clinical Research Center for Respiratory Diseases, Institute of Respiratory Medicine, Chinese Academy of Medical Sciences, Department of Pulmonary and Critical Care Medicine, Center of Respiratory Medicine, China-Japan Friendship Hospital, Beijing, China

<sup>3</sup>Department of Pulmonary and Critical Care Medicine, Affiliated Hospital of Jianghan University, Wuhan, Hubei, China

<sup>4</sup>Department of Pulmonary and Critical Care Medicine, The First Affiliated Hospital, Jiangxi Medical College Nanchang University, Nanchang, China <sup>5</sup>China-Japan Friendship Hospital, Capital Medical University, Beijing,

- <sup>6</sup>The First Clinical Medical College, Shanxi Medical University, Taiyuan, China
- <sup>7</sup>Department of Respiratory and Neurology, The Affiliated Tumor Hospital of Xinjiang Medical University, Urumqi, China
- <sup>8</sup>Institute of Clinical Medical Sciences, China-Japan Friendship Hospital, Beijing, China

<sup>9</sup>State Key Laboratory of Respiratory Health and Multimorbidity, Department of Physiology,, Institute of Basic Medical Sciences, Chinese Academy of Medical Sciences and School of Basic Medicine, Peking Union Medical College, Beijing, China

Received: 14 May 2025 / Accepted: 17 July 2025 Published online: 10 October 2025

#### References

- Humbert M, Kovacs G, Hoeper MM, et al. 2022 ESC/ERS Guidelines for the diagnosis and treatment of pulmonary hypertension. Eur Heart J. 2022;43(38):3618–731. https://doi.org/10.1093/eurheartj/ehac237.
- Elwing JM, Vaidya A, Auger WR. Chronic thromboembolic pulmonary hypertension: an update. Clin Chest Med. 2018;39(3):605–20. https://doi.org/10.1016/j.ccm.2018.04.018
- Girard P, Decousus M, Laporte S, et al. Diagnosis of pulmonary embolism in patients with proximal deep vein thrombosis: specificity of symptoms and perfusion defects at baseline and during anticoagulant therapy. Am J Respir Crit Care Med. 2001;164(6):1033–7. https://doi.org/10.1164/ajrccm.164.6.2101 045.
- Moser KM, LeMoine JR. Is embolic risk conditioned by location of deep venous thrombosis? Ann Intern Med. 1981;94(4 pt 1):439–44. https://doi.org/ 10.7326/0003-4819-94-4-439.
- van Langevelde K, Srámek A, Vincken PWJ, van Rooden JK, Rosendaal FR, Cannegieter SC. Finding the origin of pulmonary emboli with a total-body magnetic resonance direct thrombus imaging technique. Haematologica. 2013;98(2):309–15. https://doi.org/10.3324/haematol.2012.069195.
- Pang W, Zhang Z, Wang Z, et al. Higher incidence of chronic thromboembolic pulmonary hypertension after acute pulmonary embolism in asians than in europeans: a meta-analysis. Front Med (Lausanne). 2021;8:721294. https://doi. org/10.3389/fmed.2021.721294.
- Yang S, Yang Y, Zhai Z, et al. Incidence and risk factors of chronic thromboembolic pulmonary hypertension in patients after acute pulmonary embolism. J Thorac Dis. 2015;7(11):1927–38. https://doi.org/10.3978/j.issn.2072-1439.2015 .11.43.
- Luijten D, Talerico R, Barco S, et al. Incidence of chronic thromboembolic pulmonary hypertension after acute pulmonary embolism: an updated systematic review and meta-analysis. Eur Respir J. 2023;62(1):2300449. https://doi.org/10.1183/13993003.00449-2023.
- Rashidi F, Parvizi R, Bilejani E, Mahmoodian B, Rahimi F, Koohi A. Evaluation
  of the incidence of chronic thromboembolic pulmonary hypertension 1
  year after first episode of acute pulmonary embolism: a cohort study. Lung.
  2020;198(1):59–64. https://doi.org/10.1007/s00408-019-00315-3.
- Delcroix M, Torbicki A, Gopalan D, et al. ERS statement on chronic thromboembolic pulmonary hypertension. Eur Respir J. 2021;57(6):2002828. https://doi.org/10.1183/13993003.02828-2020.
- Bochenek ML, Rosinus NS, Lankeit M, et al. From thrombosis to fibrosis in chronic thromboembolic pulmonary hypertension. Thromb Haemost. 2017;117(4):769–83. https://doi.org/10.1160/TH16-10-0790.
- Alias S, Redwan B, Panzenboeck A, et al. Defective angiogenesis delays thrombus resolution: a potential pathogenetic mechanism underlying chronic thromboembolic pulmonary hypertension. Arterioscler Thromb Vasc Biol. 2014;34(4):810–9. https://doi.org/10.1161/ATVBAHA.113.302991.
- Bochenek ML, Leidinger C, Rosinus NS, et al. Activated endothelial TGFβ1 Signaling promotes venous thrombus nonresolution in mice via endothelin-1: potential role for chronic thromboembolic pulmonary hypertension. Circ Res. 2020;126(2):162–81. https://doi.org/10.1161/CIRCRESAHA.119.315259.
- Quach ME, Chen W, Li R. Mechanisms of platelet clearance and translation to improve platelet storage. Blood. 2018;131(14):1512–21. https://doi.org/10.118 2/blood-2017-08-743229.
- Lannan KL, Phipps RP, White RJ. Thrombosis, platelets, microparticles and PAH: more than a clot. Drug Discov Today. 2014;19(8):1230–5. https://doi.org/10.10 16/j.drudis.2014.04.001.

- Yaoita N, Shirakawa R, Fukumoto Y, et al. Platelets are highly activated in patients of chronic thromboembolic pulmonary hypertension. Arterioscler Thromb Vasc Biol. 2014;34(11):2486–94. https://doi.org/10.1161/ATVBAHA.11 4.304404.
- Remková A, Šimková I, Valkovičová T. Platelet abnormalities in chronic thromboembolic pulmonary hypertension. Int J Clin Exp Med. 2015;8(6):9700–7.
- Åberg M, Björklund E, Wikström G, Christersson C. Platelet-leukocyte aggregate formation and inflammation in patients with pulmonary arterial hypertension and CTEPH. Platelets. 2022;33(8):1199–207. https://doi.org/10.1 080/09537104.2022.2087867.
- Mussano F, Genova T, Munaron L, Petrillo S, Erovigni F, Carossa S. Cytokine, chemokine, and growth factor profile of platelet-rich plasma. Platelets. 2016;27(5):467–71. https://doi.org/10.3109/09537104.2016.1143922.
- Xiong G, Lingampalli N, Koltsov JCB, et al. Men and women differ in the biochemical composition of platelet-rich plasma. Am J Sports Med. 2018;46(2):409–19. https://doi.org/10.1177/0363546517740845.
- Miroshnychenko O, Chalkley RJ, Leib RD, Everts PA, Dragoo JL. Proteomic analysis of platelet-rich and platelet-poor plasma. Regen Ther. 2020;15:226– 35. https://doi.org/10.1016/j.reth.2020.09.004.
- 22. Jiang Z, Huang C, Guo E, et al. Platelet-rich plasma in young and elderly humans exhibits a different proteomic profile. J Proteome Res. 2024;23(5):1788–800. https://doi.org/10.1021/acs.jproteome.4c00030.
- Wang SL, Liu XL, Kang ZC, Wang YS. Platelet-rich plasma promotes peripheral nerve regeneration after sciatic nerve injury. Neural Regen Res. 2023;18(2):375–81. https://doi.org/10.4103/1673-5374.346461.
- Zhang Y, Zhang M, Yang H, et al. Serum proteome profiling reveals heparanase as a candidate biomarker for chronic thromboembolic pulmonary hypertension. iScience. 2024;27(2):108930. https://doi.org/10.1016/j.isci.2024. 108930.
- Szelenberger R, Jóźwiak P, Kacprzak M, et al. Variations in blood platelet proteome and transcriptome revealed altered expression of transgelin-2 in acute coronary syndrome patients. Int J Mol Sci. 2022;23(11):6340. https://doi.org/1 0.3390/ijms23116340.
- Letunica N, Van Den Helm S, McCafferty C, et al. Proteomics in thrombosis and hemostasis. Thromb Haemost. 2022;122(7):1076–84. https://doi.org/10.1 055/a-1690-8897.
- Zhang M, Li H, Ma S, et al. Serum proteome profiling reveals HGFA as a candidate biomarker for pulmonary arterial hypertension. Respir Res. 2024;25(1):418. https://doi.org/10.1186/s12931-024-03036-1.
- de Baptista Barros Ribeiro Dourado LP, Santos M, Moreira-Gonçalves D. Nets, pulmonary arterial hypertension, and thrombo-inflammation. J Mol Med. 2022;100(5):713–22. https://doi.org/10.1007/s00109-022-02197-0.
- García Á. Platelet clinical proteomics: Facts, challenges, and future perspectives. Proteomics Clin Appl. 2016;10(8):767–73. https://doi.org/10.1002/prca.201500125.
- Li B, Li G, Yang X, Song Z, Wang Y, Zhang Z. NETosis in psoriatic arthritis: serum MPO-DNA complex level correlates with its disease activity. Front Immunol. 2022;13:911347. https://doi.org/10.3389/fimmu.2022.911347.
- Koudstaal T, van den Bosch T, Bergen I, et al. Predominance of M2 macrophages in organized thrombi in chronic thromboembolic pulmonary hypertension patients. Eur J Immunol. 2024;54(6):e2350670. https://doi.org/10.1002/eji.202350670.
- Quarck P, Wynants M, Ronisz A, et al. Characterization of proximal pulmonary arterial cells from chronic thromboembolic pulmonary hypertension patients. Respir Res. 2012;13(1):27. https://doi.org/10.1186/1465-9921-13-27.
- Sharma S, Hofbauer TM, Ondracek AS, et al. Neutrophil extracellular traps promote fibrous vascular occlusions in chronic thrombosis. Blood. 2021;137(8):1104–16. https://doi.org/10.1182/blood.2020005861.
- Altmayer SPL, Han QJ, Addetia K, Patel AR, Forfia PR, Han Y. Using all-cause mortality to define severe RV dilation with RV/LV volume ratio. Sci Rep. 2018;8(1):7200. https://doi.org/10.1038/s41598-018-25259-1.
- Colalillo A, Hoffmann-Vold AM, Pellicano C, et al. The role of TAPSE/sPAP ratio in predicting pulmonary hypertension and mortality in the systemic sclerosis EUSTAR cohort. Autoimmun Rev. 2023. https://doi.org/10.1016/j.autrev.2023. 103290
- Çolak A, Kumral Z, Kış M, et al. The usefulness of the TAPSE/sPAP ratio for predicting survival in medically treated chronic thromboembolic pulmonary hypertension. Turk Kardiyol Dern Ars. 2023;51(7):470–7. https://doi.org/10.554 3/tkda.2023.78074.
- Banfi C, Brioschi M, Marenzi G, et al. Proteome of platelets in patients with coronary artery disease. Exp Hematol. 2010;38(5):341–50. https://doi.org/10.1 016/j.exphem.2010.03.001.

- Parguiña AF, Grigorian-Shamajian L, Agra RM, et al. Proteins involved in platelet signaling are differentially regulated in acute coronary syndrome: a proteomic study. PLoS ONE. 2010;5(10):e13404. https://doi.org/10.1371/journ al.pone.0013404.
- Etulain J. Platelets in wound healing and regenerative medicine. Platelets. 2018;29(6):556–68. https://doi.org/10.1080/09537104.2018.1430357.
- Everts PAM, Knape JTA, Weibrich G, et al. Platelet-rich plasma and platelet gel: a review. J Extra Corpor Technol. 2006;38(2):174–87.
- Vu TD, Pal SN, Ti LK, et al. An autologous platelet-rich plasma hydrogel compound restores left ventricular structure, function and ameliorates adverse remodeling in a minimally invasive large animal myocardial restoration model: a translational approach: Vu and Pal "Myocardial Repair: PRP, Hydrogel and Supplements." Biomaterials. 2015;45:27–35. https://doi.org/10.1016/j.biomaterials.2014.12.013.
- Martínez CE, González SA, Palma V, Smith PC. Platelet-poor and platelet-rich plasma stimulate bone lineage differentiation in periodontal ligament stem cells. J Periodontol. 2016;87(2):e18-26. https://doi.org/10.1902/jop.2015.1503 60.
- Gao X, Zhao X, Li J, et al. Neutrophil extracellular traps mediated by platelet microvesicles promote thrombosis and brain injury in acute ischemic stroke. Cell Commun Signal:CCS. 2024. https://doi.org/10.1186/s12964-023-01379-8.
- 44. Vogel S, Rath D, Borst O, et al. Platelet-derived high-mobility group box 1 promotes recruitment and suppresses apoptosis of monocytes. Biochem Biophys Res Commun. 2016;478(1):143–8. https://doi.org/10.1016/j.bbrc.2016
- Jiao Y, Li W, Wang W, et al. Platelet-derived exosomes promote neutrophil extracellular trap formation during septic shock. Crit Care. 2020;24(1):380. htt ps://doi.org/10.1186/s13054-020-03082-3.
- Vogel S, Bodenstein R, Chen Q, et al. Platelet-derived HMGB1 is a critical mediator of thrombosis. J Clin Invest. 2015;125(12):4638–54. https://doi.org/1 0.1172/JCI81660.
- Kim SJ, Jenne CN. Role of platelets in neutrophil extracellular trap (NET) production and tissue injury. Semin Immunol. 2016;28(6):546–54. https://doi. org/10.1016/j.smim.2016.10.013.
- Fang X, Zhou X, Zhou X, Cheng Z, Hu Y. HMGB1-platelet interactions: mechanisms and targeted therapy strategies. Thromb Haemost. 2025. https://doi.org/10.1055/a-2622-0074
- Walsh TG, Berndt MC, Carrim N, Cowman J, Kenny D, Metharom P. The role of Nox1 and Nox2 in GPVI-dependent platelet activation and thrombus formation. Redox Biol. 2014;2:178–86. https://doi.org/10.1016/j.redox.2013.12.023.
- Chlopicki S, Olszanecki R, Janiszewski M, Laurindo FRM, Panz T, Miedzobrodzki J. Functional role of NADPH oxidase in activation of platelets.
   Antioxid Redox Signal. 2004;6(4):691–8. https://doi.org/10.1089/15230860413 61640
- 51. Seno T, Inoue N, Gao D, et al. Involvement of NADH/NADPH oxidase in human platelet ROS production. Thromb Res. 2001;103(5):399–409. https://doi.org/10.1016/s0049-3848(01)00341-3.
- Kim K, Li J, Tseng A, Andrews RK, Cho J. NOX2 is critical for heterotypic neutrophil-platelet interactions during vascular inflammation. Blood. 2015;126(16):1952–64. https://doi.org/10.1182/blood-2014-10-605261.
- Zamolodchikova TS, Tolpygo SM, Svirshchevskaya EV. Cathepsin G-Not only inflammation: the immune protease can regulate normal physiological processes. Front Immunol. 2020;11:411. https://doi.org/10.3389/fimmu.2020. 00411
- Taylor S, Dirir O, Zamanian RT, Rabinovitch M, Thompson AAR. The role of neutrophils and neutrophil elastase in pulmonary arterial hypertension. Front Med (Lausanne). 2018;5:217. https://doi.org/10.3389/fmed.2018.00217.
- Molino M, Blanchard N, Belmonte E, et al. Proteolysis of the human platelet and endothelial cell thrombin receptor by neutrophil-derived cathepsin G. J Biol Chem. 1995;270(19):11168–75. https://doi.org/10.1074/jbc.270.19.11168.

- Papayannopoulos V. Neutrophil extracellular traps in immunity and disease. Nat Rev Immunol. 2018;18(2):134–47. https://doi.org/10.1038/nri.2017.105.
- Wang Y, Wysocka J, Sayegh J, et al. Human PAD4 regulates histone arginine methylation levels via demethylimination. Science. 2004;306(5694):279–83. h ttps://doi.org/10.1126/science.1101400.
- Tsourouktsoglou TD, Warnatsch A, Ioannou M, Hoving D, Wang Q, Papayannopoulos V. Histones, DNA, and citrullination promote neutrophil extracellular trap inflammation by regulating the localization and activation of TLR4. Cell Rep. 2020;31(5):107602. https://doi.org/10.1016/j.celrep.2020.107602.
- Aldabbous L, Abdul-Salam V, McKinnon T, et al. Neutrophil extracellular traps promote angiogenesis: evidence from vascular pathology in pulmonary hypertension. Arterioscler Thromb Vasc Biol. 2016;36(10):2078–87. https://doi. org/10.1161/ATVBAHA.116.307634.
- Perdomo J, Leung HHL, Ahmadi Z, et al. Neutrophil activation and NETosis are the major drivers of thrombosis in heparin-induced thrombocytopenia. Nat Commun. 2019;10(1):1322. https://doi.org/10.1038/s41467-019-09160-7.
- Gollomp K, Kim M, Johnston I, et al. Neutrophil accumulation and NET release contribute to thrombosis in HIT. JCI Insight. 2018;3(18):e99445. https://doi.org/10.1172/jci.insight.99445.
- Holinstat M. Normal platelet function. Cancer Metastasis Rev. 2017;36(2):195– 8. https://doi.org/10.1007/s10555-017-9677-x.
- Koupenova M, Clancy L, Corkrey HA, Freedman JE. Circulating platelets as mediators of immunity, inflammation, and thrombosis. Circ Res. 2018;122(2):337–51. https://doi.org/10.1161/CIRCRESAHA.117.310795.
- Frenette PS, Denis CV, Weiss L, et al. P-Selectin glycoprotein ligand 1 (PSGL-1) is expressed on platelets and can mediate platelet-endothelial interactions in vivo. J Exp Med. 2000;191(8):1413–22. https://doi.org/10.1084/jem.191.8.141
- Smyth SS, Reis ED, Zhang W, Fallon JT, Gordon RE, Coller BS. Beta(3)-integrindeficient mice but not P-selectin-deficient mice develop intimal hyperplasia after vascular injury: correlation with leukocyte recruitment to adherent platelets 1 hour after injury. Circulation. 2001;103(20):2501–7. https://doi.org/ 10.1161/01.cir.103.20.2501.
- van der Meijden PEJ, Heemskerk JWM. Platelet biology and functions: new concepts and clinical perspectives. Nat Rev Cardiol. 2019;16(3):166–79. https://doi.org/10.1038/s41569-018-0110-0.
- Li J, Kim K, Jeong SY, et al. Platelet protein disulfide isomerase promotes glycoprotein lba-mediated platelet-neutrophil interactions under thromboinflammatory conditions. Circulation. 2019;139(10):1300–19. https://doi.or g/10.1161/CIRCULATIONAHA.118.036323.
- Caillon A, Trimaille A, Favre J, Jesel L, Morel O, Kauffenstein G. Role of neutrophils, platelets, and extracellular vesicles and their interactions in COVID-19-associated thrombopathy. J Thromb Haemost. 2022;20(1):17–31. https://doi.org/10.1111/jth.15566.
- Viswanathan G, Kirshner HF, Nazo N, et al. Single-cell analysis reveals distinct immune and smooth muscle cell populations that contribute to chronic thromboembolic pulmonary hypertension. Am J Respir Crit Care Med. 2023. https://doi.org/10.1164/rccm.202203-0441OC.
- Stadler SC, Vincent CT, Fedorov VD, et al. Dysregulation of PAD4-mediated citrullination of nuclear GSK3β activates TGF-β signaling and induces epithelial-to-mesenchymal transition in breast cancer cells. Proc Natl Acad Sci U S A. 2013;110(29):11851–6. https://doi.org/10.1073/pnas.1308362110.

### **Publisher's Note**

Springer Nature remains neutral with regard to jurisdictional claims in published maps and institutional affiliations.